


## Article

# Facile Synthesis of Hollow V<sub>2</sub>O<sub>5</sub> Microspheres for Lithium-Ion Batteries with Improved Performance

Hailong Fei <sup>1,\*</sup>, Peng Wu <sup>1</sup>, Liqing He <sup>2,3,\*</sup> and Haiwen Li <sup>2,3</sup> 

<sup>1</sup> State Key Laboratory of Photocatalysis on Energy and Environment, College of Chemistry, Fuzhou University, Fuzhou 350108, China

<sup>2</sup> Hefei General Machinery Research Institute Co., Ltd., Hefei 230031, China; lihaiwen66@hotmail.com

<sup>3</sup> Anhui Provincial Laboratory of Technology for Hydrogen Storage and Transportation Equipment, Hefei 230031, China

\* Correspondence: hailongfei@fzu.edu.cn (H.F.); heli\_limao@163.com (L.H.)

**Abstract:** Micro-nanostructured electrode materials are characterized by excellent performance in various secondary batteries. In this study, a facile and green hydrothermal method was developed to prepare amorphous vanadium-based microspheres on a large scale. Hollow V<sub>2</sub>O<sub>5</sub> microspheres were achieved, with controllable size, after the calcination of amorphous vanadium-based microspheres and were used as cathode materials for lithium-ion batteries. As the quantity of V<sub>2</sub>O<sub>5</sub> microspheres increased, the electrode performance improved, which was ascribed to the smaller charge transfer impedance. The discharge capacity of hollow V<sub>2</sub>O<sub>5</sub> microspheres could be up to 196.4 mAhg<sup>-1</sup> at a current density of 50 mA g<sup>-1</sup> between 2.0 and 3.5 V voltage limits. This sheds light on the synthesis and application of spherical electrode materials for energy storage.

**Keywords:** microsphere; lithium-ion battery; vitamin C; vanadium acetylacetonate; hydrothermal



**Citation:** Fei, H.; Wu, P.; He, L.; Li, H. Facile Synthesis of Hollow V<sub>2</sub>O<sub>5</sub> Microspheres for Lithium-Ion Batteries with Improved Performance. *Inorganics* **2024**, *12*, 37. <https://doi.org/10.3390/inorganics12020037>

Academic Editors: Rainer Niewa, Pengwei Li and Shaohua Luo

Received: 11 December 2023

Revised: 22 January 2024

Accepted: 22 January 2024

Published: 24 January 2024



**Copyright:** © 2024 by the authors. Licensee MDPI, Basel, Switzerland. This article is an open access article distributed under the terms and conditions of the Creative Commons Attribution (CC BY) license (<https://creativecommons.org/licenses/by/4.0/>).

## 1. Introduction

It is important to explore lithium-ion batteries with high energy density and safety because they have achieved great commercial success in portable devices and electric vehicles [1]. Vanadium oxide (V<sub>2</sub>O<sub>5</sub>) is a fascinating material due to its high energy density, layer structure, and rich abundance. It has been widely reported in the photocatalytic degradation of gaseous o-dichlorobenzene [2] and metal-ion batteries, such as lithium-ion [3], sodium-ion, potassium-ion, magnesium-ion, and lithium–sulfur batteries. Flowerlike hollow V<sub>2</sub>O<sub>5</sub> microspheres with diameters of about 700–800 nm with carbon spheres as templates were achieved, and they could photodegrade o-DCB to o-benzoquinone-type and organic acid species under visible light due to their strong adsorption capacity and large specific surface area [2]. In addition, hollow V<sub>2</sub>O<sub>5</sub> microspheres consisting of closely packed particles, radially aligned rods, and randomly packed platelets were achieved by calcining the as-synthesized precursors prepared with NH<sub>4</sub>VO<sub>3</sub>, oxalic acid, and tetrahydrofuran. The hollow V<sub>2</sub>O<sub>5</sub> microspheres consisting of randomly packed platelets showed the highest activity in degrading rhodamine B under UV light by enhancing UV light absorbance [4]. Beta-V<sub>2</sub>O<sub>5</sub> with a layered structure, obtained through a high-temperature and high-pressure method, showed a high capacity of 147 mAh g<sup>-1</sup> under equilibrium conditions, corresponding to the insertion of 1 Na<sup>+</sup> per formula unit in the 2.0–3.6 V range at a C/20 current density [5]. Delta-K<sub>0.51</sub>V<sub>2</sub>O<sub>5</sub> nanobelts reconstructed from orthorhombic V<sub>2</sub>O<sub>5</sub> polyhedra showed a high average voltage (3.2 V), high capacity (131 mAhg<sup>-1</sup>), and superior rate capability, even at 10 A g<sup>-1</sup>, due to their large interlayered structure [6]. Beta-V<sub>2</sub>O<sub>5</sub> has a reversible capacity of 361 mAhg<sup>-1</sup> for magnesium-ion batteries at room temperature [7]. Defect-rich W- or Mo-doped V<sub>2</sub>O<sub>5</sub> yolk–shell microspheres afford sufficient active sites to chemically anchor polysulfides with a promising catalytic effect on the

mutual conversion between different sulfur intermediates, which delivers a discharging capacity of  $1143.3 \text{ mAg}^{-1}$  at an initial rate of  $0.3 \text{ C}$  and  $681.8 \text{ mAg}^{-1}$  at  $5 \text{ C}$  [8].

Recently, modified  $\text{V}_2\text{O}_5$  has shown high capacity and long cycling stability in various next-generation aqueous rechargeable batteries, for example, aqueous zinc-ion [9,10], aluminum-ion [11], ammonium-ion [12], potassium-ion [13], iron [14], and Pb-ion batteries [15]. Commercial  $\text{V}_2\text{O}_5$  electrodes of aqueous zinc-ion batteries showed a reversible capacity of  $470 \text{ mAhg}^{-1}$  at  $0.2 \text{ Ag}^{-1}$  and long-term cyclability with 91.1% capacity retention over 4000 cycles at a current density of  $5 \text{ Ag}^{-1}$ . The co-intercalated  $\text{H}_2\text{O}$  shields the electrostatic interactions between  $\text{Zn}^{2+}$  and the host framework, accounting for the enhanced kinetics. In addition, the pristine bulk  $\text{V}_2\text{O}_5$  gradually evolves into porous nanosheets upon cycling, providing more active sites for  $\text{Zn}^{2+}$  storage [10]. An interconnected sheetlike  $\text{V}_2\text{O}_5$  structure with slight  $\text{V}_2\text{O}_5$  lattice expansion (approximately 1.4%) was reported as a cathode material for aluminum-ion batteries, delivering an initial discharge capacity of  $140 \text{ mAhg}^{-1}$  at a high current density of  $0.5 \text{ Ag}^{-1}$ , with an excellent capacity retention rate of 96% after 1000 cycles at a current density of  $1 \text{ Ag}^{-1}$  [11].  $\text{V}_2\text{O}_5$  intercalated with polyaniline showed a high capacity of  $192.5 \text{ mAhg}^{-1}$  and  $39 \text{ mAhg}^{-1}$  at specific currents of 1 and  $20 \text{ Ag}^{-1}$ , respectively, as well as a stable cycle life, with a capacity retention rate of 98% at a specific current of 10 and  $20 \text{ Ag}^{-1}$  due to the improved kinetics in aqueous ammonium-ion batteries [12]. The Pb/ $\text{V}_2\text{O}_5$  battery showed a voltage of 0.44 V and a capacity of  $162.6 \text{ mAhg}^{-1}$  with a capacity retention rate of 87.5% after 150 cycles [15]. However, the low discharge voltage, low conductivity, and irreversible phase conversion of  $\text{V}_2\text{O}_5$  reduce the stability of the material and restrict its application on a large scale. Three-dimensional nanostructures with internal vacancies have mitigated these drawbacks due to buffer volume expansion, reducing the stress and strain caused by the insertion/extraction of lithium ion and providing a shorter  $\text{Li}^+$  diffusion distance [16]. It was reported that spherelike electrode materials of vanadium oxides [17,18] with low free energy showed better electrode performance than their bulk counterpart for the positive contribution of the ion and electron transfer.  $\text{V}_2\text{O}_5$  microspheres were obtained after annealing uniform  $\text{VO}_2$  microspheres with various complex interiors, such as yolk-shell and multishelled hollow structures. Yolk-shell  $\text{V}_2\text{O}_5$  microspheres were found to have a specific capacity of  $140 \text{ mAhg}^{-1}$ , with no fading over 100 cycles. Nanoscale building blocks in the core and the shell enhanced the transport of lithium ions, and electrons and void space within the microspheres and the porous shell ensured efficient electrolyte penetration and increased the contact area between the electrode and electrolyte [17]. To date,  $\text{V}_2\text{O}_5$  microspheres have been prepared via the following methods, with the aid of surfactants and hard templates, the polyol process, and solvothermal and hydrothermal reduction. Ethylene glycol (EG), which is an important member of the polyol family, has been used to prepare complex hollow  $\text{V}_2\text{O}_5$  microspheres as a cross-linking reagent by changing the moiety of reactants, such as ammonium metavanadate ( $\text{NH}_4\text{VO}_3$ ) [19], citric acid and  $\text{NH}_4\text{VO}_3$  [20],  $\text{NH}_4\text{VO}_3$  and nickel acetate [21],  $\text{VOC}_2\text{O}_4$  [22], vanadium (IV) acetylacetonate [23], and vanadyl glycolates [24]. Nanostructured hollow  $\text{V}_2\text{O}_5$  microspheres were obtained after subsequent calcination of hollow nanostructured vanadyl glycolate microspheres that were prepared via a polyol-induced solvothermal process through self-seeding and then aggregated around  $\text{N}_2$  microbubbles. These hollow  $\text{V}_2\text{O}_5$  microspheres showed excellent cycle stability and high-rate performance, which were attributed to the relatively thin-walled structure that ensured fast phase penetration between the electrolyte and active material and shortened the lithium-ion migration distance [19]. Hollow vanadium pentoxide ( $\text{V}_2\text{O}_5$ ) microspheres with mesopores on the shell were obtained after the calcination of vanadium precursors prepared with citric acid, ammonium metavanadate, and ethylene glycol, achieving a reversible capacity of  $710.2 \text{ mAhg}^{-1}$  after 400 cycles at a current density of  $0.5 \text{ Ag}^{-1}$  between 0 and 3.5 V voltage limits, providing channels for electrolyte transfer [20]. Hollow  $\text{V}_2\text{O}_5$  microspheres were prepared via a nickel-mediated polyol process, in which nickel acts not only as a mediator to tailor the interior hollow structures of  $\text{V}_2\text{O}_5$  and build favorable 3D hierarchical combined nano- and microarchitecture but also as doping

units to tune vanadium's valence states and improve the lithium storage properties [21]. Three-dimensional (3D) hollow vanadium pentoxide (the precursor hollow microflowers were first prepared from a solution of vanadium oxytriisopropoxide (VOT) in isopropyl alcohol (IPA) via a one-step solvothermal treatment). Nano-/microspheres were fabricated via the one-step solvothermal treatment of  $V_2O_5$ , oxalic acid, and ethylene glycol followed by annealing [22].  $V_2O_5$  microspheres with hierarchical structure were obtained via the subsequent thermal annealing treatment of a vanadium glycolate precursor prepared through a template-free process in a polyol medium [23]. Further, 3–6  $\mu\text{m}$  hierarchical and porous  $V_2O_5$  microspheres constructed of intertwined laminar nanocrystals or cross-linked nanobricks have been fabricated by a refluxing approach followed by annealing vanadium glycolates in air. The porous  $V_2O_5$  microspheres assembled from intertwined nanoparticles maintain reversible  $\text{Li}^+$  storage capacities of 102 and 80  $\text{mAh g}^{-1}$ , respectively [24]. An organic vanadium source will accumulate microspheres under these conditions. After calcination, various hollow  $V_2O_5$  microspheres accumulated from rodlike particles were obtained, with low surface areas. The solvothermal process is also an effective way to prepare spherelike precursors. Uniform  $V_2O_5$  nanosheet-assembled hollow microflowers [25], rigid  $V_2O_5$  microspheres [26], yolk-shell  $V_2O_5$  microspheres [27], and internal diffusion [28] can be prepared with vanadium oxytriisopropoxide (VOT), vanadyl citrate ( $\text{VOC}_6\text{H}_6\text{O}_7$ ),  $V_2O_5$ , a mixture of ammonium metavanadate ( $\text{NH}_4\text{VO}_3$ ) and glucose in isopropanol alcohol (IPA), or a mixed solvent of glycerol and isopropanol, respectively. Hollow microflowers were first prepared from a solution of vanadium oxytriisopropoxide (VOT) in isopropyl alcohol (IPA) via a one-step solvothermal treatment, and they could be easily converted to hierarchical hollow  $V_2O_5$  microflowers composed of nanosheet alterations via simple annealing [25]. Nanoparticle-assembled, rigid, hollow  $V_2O_5$  microspheres were prepared through solvothermal treatment of vanadyl citrate in isopropanol and subsequent calcination, showing a maximum specific discharge capacity of 128  $\text{mAhg}^{-1}$  at 1  $\text{Ag}^{-1}$  within a voltage window of 2.5 to 4 V for lithium-ion batteries [26]. The solid, yolk-shell, and hollow  $V_2O_5$  microspheres were successfully prepared in a mixed solvent containing isopropanol, with carbon spheres as a template, through an annealing treatment in air. Hollow  $V_2O_5$  microspheres showed better electrochemical performance than solid or yolk-shell microspheres, which was attributed to the fact that the thin porous shell and hollow interior allowed easy penetration by the electrolyte and rapid diffusion of ions, ensuring that full use was made of the active  $V_2O_5$  material during the  $\text{Li}^+$  insertion/extraction process [27]. Hollow  $V_2O_5$  microspheres whose hierarchical shell thicknesses were changed by controlling the internal diffusion rate of the glucose-derived carbon core precursor were prepared using a simple solvothermal method and a subsequent annealing process, which delivered a high reversible specific capacity of 287  $\text{mAhg}^{-1}$  at 1/3 C with good cycling stability due to the full contact with the electrolyte, with shortened ion diffusion paths, alleviating the volume change in the charge/discharge process via self-created pores [28]. Hollow sphere particles with a diameter of 0.7–1.6  $\mu\text{m}$  were fabricated with ethanol, ammonium vanadate, and nitric acid, and they displayed a high specific discharge capacity of 132  $\text{mAhg}^{-1}$  with a capacity retention rate of 82.5% after 6200 cycles at a current density of 10  $\text{Ag}^{-1}$  [29]. Porous monodispersed  $V_2O_5$  microspheres were prepared with  $\text{VO}(\text{OiPr})_3$  and pyridine/acetone/ $\text{H}_2\text{O}$  through sequent reduction/oxidation treatment at a high temperature, and the formation of pores was due to the release of pyridine, which shows excellent low-temperature behavior, with a reversible capacity of 102  $\text{mAhg}^{-1}$  at  $-20$  degrees due to a large interfacial contact area with the electrolyte caused by the porous structure of  $V_2O_5$  spheres [30].

As we know, the shape and size of the building blocks, the surface area, the pore size, and the sphere shell's thickness all have important effects on the cycling stability and discharge capacity of hollow  $V_2O_5$  microspheres. Suitable surfactants can be used to adjust these characteristics. Self-assembly of  $V_2O_5$  nanorods into microspheres was mediated by a polyol process in the presence of poly(vinylpyrrolidone) (PVP) [31]. Hollow  $V_2O_5$  microspheres with pores (HPVOM) can be obtained through a facile poly(vinylpyrrolidone)-

and ethylene-glycol-assisted soft-template solvothermal method, which, in this study, exhibited  $407.9 \text{ mAhg}^{-1}$  at a current density of  $1.0 \text{ Ag}^{-1}$  after 700 cycles, and the full  $\text{LiFePO}_4/\text{HPVOM}$  cell had a discharge capacity of  $109.9 \text{ mAhg}^{-1}$  after 150 cycles at  $0.1 \text{ Ag}^{-1}$  [32]. Hollow  $\text{V}_2\text{O}_5$  microspheres built from nanocuboids and nanoplatelets were achieved by splitting PVP-based micelles and enhancing the movement of chains in PVP. The hollow  $\text{V}_2\text{O}_5$  microspheres made up of nano-platelets showed a higher discharge capacity ( $292 \text{ mA h/g}$  at  $44.5 \text{ mA/g}$ ) and better rate performance than the microspheres built of nano-cuboids. This is attributable to the improved surface area, agglomeration resistance, and short diffusion path of lithium ions in nanoscale 2D  $\text{V}_2\text{O}_5$  platelets [33]. Hollow  $\text{V}_2\text{O}_5$  nanospheres with an average diameter of 28 nm and a hollow cavity size of approximately 18 nm were prepared by using polymeric micelles of polymer poly(styrene-*b*-2-vinyl-1-methylpyridinium iodide-*b*-ethylene oxide) (PS-PVMP-PEO) in DMF containing 10 wt% water as a soft template after calcination at  $500 \text{ }^\circ\text{C}$ ; these nanospheres maintained their structural integrity, even after being subjected to a high current density of  $2000 \text{ Ag}^{-1}$ , and showed good cycling performance, which was attributed to the nanosize effect coupled with the hollow void space of the hollow  $\text{V}_2\text{O}_5$  particles that facilitated fast lithium intercalation/deintercalation [34]. With the increasing interest in  $\text{V}_2\text{O}_5$  in the field of rechargeable batteries, there is an urgent need to develop a green, convenient, low-cost, and freely available organic solvent synthesis technology for microspheres of substances such as vanadium pentoxide. Hierarchical  $\text{V}_2\text{O}_5$  sub-microspheres composed of stacked platelets were prepared via precipitation of a  $\text{V}(\text{OH})_2\text{NH}_2$  precursor in aqueous solution and subsequent calcination; the resulting structures showed a high capacity of  $266 \text{ m hg}^{-1}$  and good cycling stability ( $200 \text{ mAhg}^{-1}$  after 100 cycles) at a current density of  $300 \text{ mAg}^{-1}$  as cathode materials for lithium-ion batteries [35]. Hollow and porous  $\text{V}_2\text{O}_5$  microspheres can be prepared through a spray pyrolysis process with  $\text{V}_2\text{O}_5$  and sucrose solution [36,37]. Sponge-like  $\text{V}_2\text{O}_5$  was obtained via the calcination of nanostructured amorphous tetrabutylammonium decavanadate arrays containing  $[\text{V}_{10}\text{O}_{28}]_6$  decavanadate anions with a dicationic Gemini surfactant, achieving higher initial capacity and better capacity retention than the more agglomerated  $\text{V}_2\text{O}_5$  consisting of very small crystallites [4]. Here, we developed a facile method to prepare amorphous vanadium-based microspheres. After the calcination of amorphous vanadium-based microspheres,  $\text{V}_2\text{O}_5$  microspheres with controllable size were obtained.  $\text{V}_2\text{O}_5$  microspheres were tested as cathode materials for lithium-ion batteries. The  $\text{V}_2\text{O}_5$  microspheres' performance could be improved by adjusting their size. When the  $\text{V}_2\text{O}_5$  microspheres were smaller, their cycling stability was better.

## 2. Results and Discussion

### 2.1. Morphologies of Materials

Ascorbic acid plays an important role in obtaining spherical vanadium precursors. Only nanoparticles below 200 nm were obtained in the absence of ascorbic acid, as shown in Figure 1a,b. When the molar ratio of vanadium acetylacetonate to ascorbic acid was 1:5, monodispersed microspheres of approximately  $1 \mu\text{m}$  were obtained, as shown in Figure 1c. The magnified SEM images show that the coarse surface of the microspheres was covered with nanoparticles, as shown in Figure 1d. The microspheres became larger with increasing amounts of ascorbic acid, and the same was true of the nanoparticles on the surface. When the molar ratio of vanadium acetylacetonate to ascorbic acid was 1:10, microspheres covered with nanoparticles were achieved, as shown in Figure 1e. The magnified SEM images show that there were two kinds of nanoparticles on the surface. The larger plateletlike nanoparticles were less numerous than the smaller nanoparticles in Figure 1f.

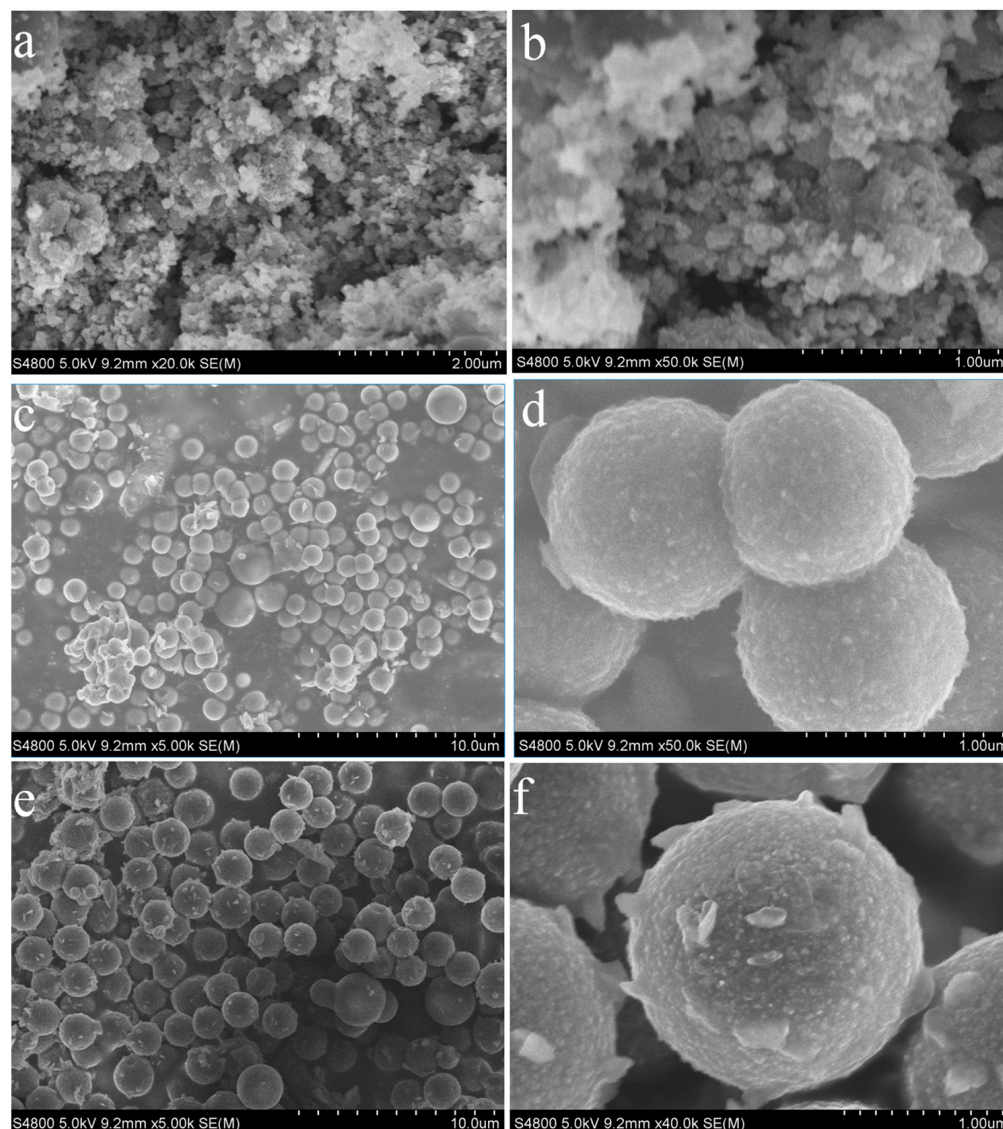


**Figure 1.** SEM images of vanadium precursors prepared at different molar ratios of vanadium acetylacetonate to ascorbic acid: (a,b) 1:0, (c,d) 1:5, and (e,f) 1:10.

To test the thermal stability of the as-synthesized vanadium precursors, all the precursors were calcined at 400 °C for 2 h in air. It could be seen that nanoparticles prepared without ascorbic acid were accumulated into large blocks, shown in Figure 2a. The magnified SEM images show that nanorods were obtained, as can be seen in Figure 2b. Monodispersed microspheres were still obtained for the precursors prepared with a molar ratio of vanadium acetylacetonate to ascorbic acid of 1:5. The average size of the microspheres was approximately 1  $\mu\text{m}$ , as shown in Figure 2c. The appearance of some broken microspheres confirmed that they were hollow. The magnified SEM images further show that the hollow microspheres were built with small particles, as shown in Figure 2d. The thickness of the microspheres was approximately 340 nm. With increasing amounts ascorbic acid, the thermal stability of microspheres dropped dramatically. Some microspheres were broken, as shown in Figure 2e. The magnified SEM images show that there were rod-like nanoparticles on the surface of hollow microspheres, as in Figure 2f. The size of the hollow  $\text{V}_2\text{O}_5$  microspheres was approximately 2  $\mu\text{m}$ . On the basis of the above experimental results, we propose that amorphous vanadium-based microspheres are formed via Ostwald ripening, in which primary crystals are reorganized to microspheres with the minimum surface free energy. After calcination, the as-synthesized precursors retain the original spherelike morphologies.

The nanoparticles in the microspheres can grow larger and larger, assembling themselves into spheres and being released in the interior to form a hollow structure.

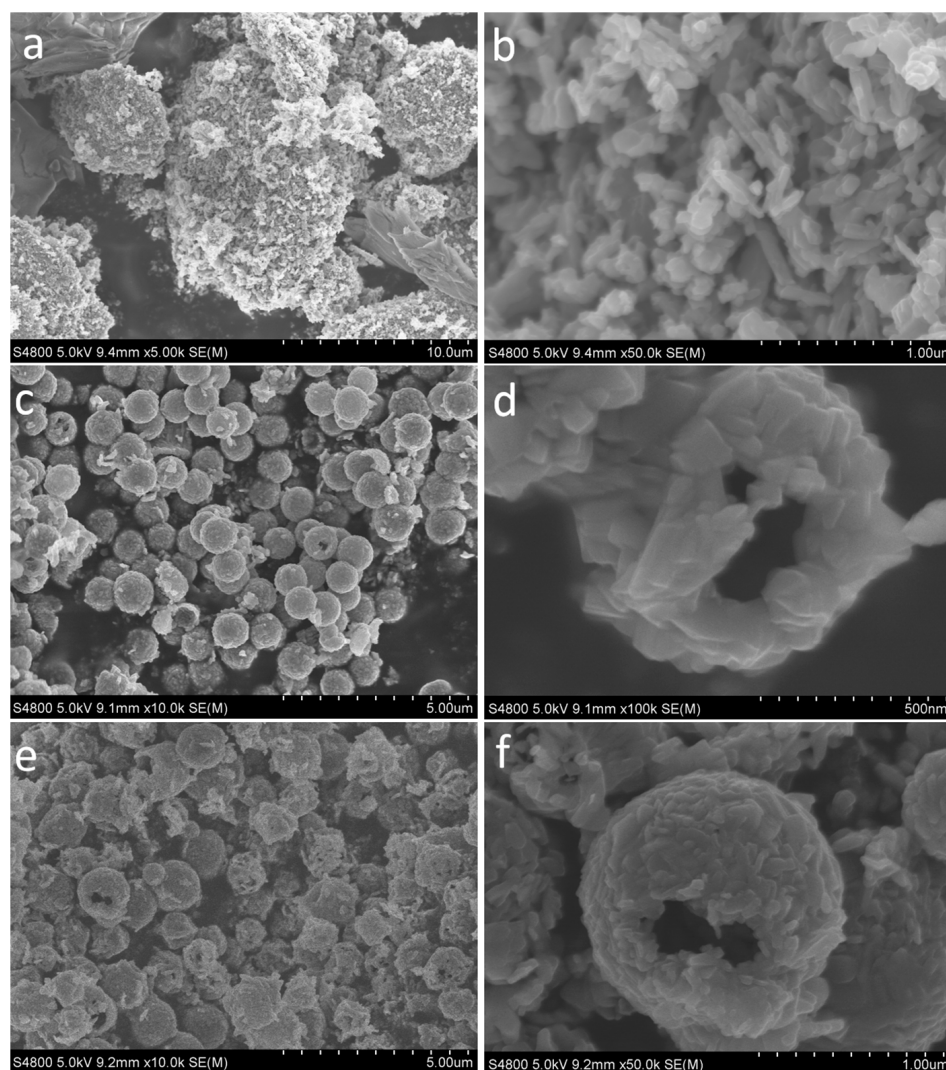


**Figure 2.** SEM images of the calcined vanadium precursors prepared at different molar ratio of vanadium acetylacetonate to ascorbic acid: (a,b) 1:0, (c,d) 1:5, and (e,f) 1:10.

## 2.2. Structure of Materials

X-ray diffraction was further performed to investigate the crystalline structure of samples. There were two small peaks at  $36.74^\circ$  and  $41.33^\circ$  for the precursor prepared without ascorbic acid (Figure 3a). They cannot be ascribed to vanadium oxides and salts. It is obvious that the as-synthesized nanoparticles were not amorphous. With the introduction of ascorbic acid into the experimental procedure, the peaks at  $36.74^\circ$  and  $41.33^\circ$  became very weak at a molar ratio of vanadium acetylacetonate to ascorbic acid of 1:5 (Figure 3b). They completely disappeared at a molar ratio of vanadium acetylacetonate to ascorbic acid of 1:10 (Figure 3c). It can be seen that ascorbic acid can inhibit the formation of crystalline vanadium-based precursors. In addition, ascorbic acid is a reducing agent that can reduce  $V^{5+}$  to  $V^{4+}$ . Thus, it can prevent  $V^{4+}$  from converting to  $V^{5+}$ , though it cannot easily form  $V_2O_5$ . The coordination effect of ascorbic acid results in the formation of two complexes, for example, vanadium (IV) L-ascorbate complexes and the vanadium (IV) dehydroascorbic acid complex [38]. The coordination effect of ascorbic acid plays an important role in the formation of sphere-like vanadium precursors. Either crystalline or amorphous microspheres can be prepared via hydrothermal synthesis. With the aid

of tetrahydrofuran, we also prepared crystalline  $\text{VO}_2$  microspheres under solvothermal conditions [4]. After calcination, all the as-synthesized samples were converted to  $\text{V}_2\text{O}_5$  (JCPDS 3-0207) in Figure 4a, b and c. Based on the above results, approximately 1 to 2  $\mu\text{m}$  hollow  $\text{V}_2\text{O}_5$  microspheres built with nanorods were achieved.

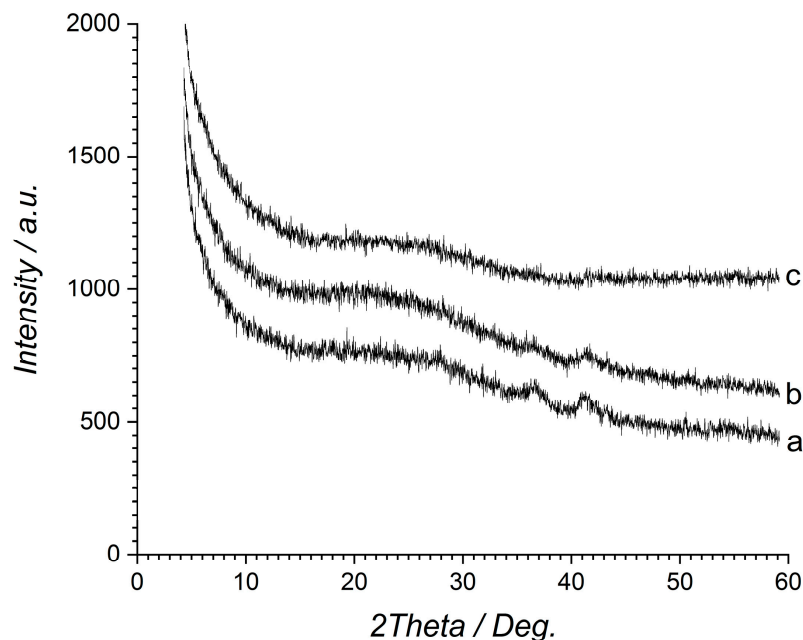


**Figure 3.** XRD patterns of as-synthesized samples prepared with different molar ratios of vanadium acetylacetonate to ascorbic acid: (a) 1:0, (b) 1:5, and (c) 1:10.

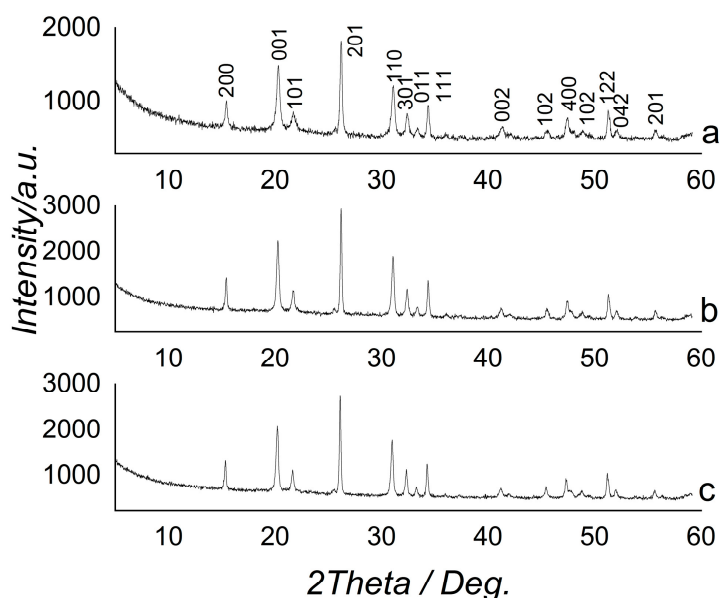


**Figure 4.** XRD patterns of the samples calcined at 400 °C after being prepared with different molar ratios of vanadium acetylacetonate to ascorbic acid: (a) 1:0, (b) 1:5, and (c) 1:10.

### 2.3. Electrochemical Performance of Materials

Cyclic voltammetry (CV) was performed to investigate the lithium intercalation for hollow  $\text{V}_2\text{O}_5$  microspheres. Figure 5a shows a cyclic voltammogram (CV) of hollow  $\text{V}_2\text{O}_5$  microspheres prepared at a molar ratio of vanadium acetylacetonate to ascorbic acid of 1:5. There were three pairs of reduction–oxidation peaks. The first pair was at (2.15, 2.52), (2.20, 2.52), (2.21, 2.52), and (2.23, 2.52) for the first, second, third, and fourth cycles,

respectively. The second and third pairs of peaks were centered at (3.13, 3.28) and (3.35, 3.48) for all four cycles. The cathodic intercalation peaks at 2.15, 3.13, and 3.35 are ascribed to  $\gamma$ - $\text{Li}_2\text{V}_2\text{O}_5$ ,  $\delta$ - $\text{LiV}_2\text{O}_5$ , and  $\epsilon$ - $\text{Li}_{0.5}\text{V}_2\text{O}_5$ , respectively, while the anodic deintercalation peaks at 2.52, 3.28, and 3.48 V are ascribed to phase transitions from  $\gamma$ - $\text{Li}_2\text{V}_2\text{O}_5$  to  $\delta$ - $\text{Li}_{0.5}\text{V}_2\text{O}_5$ ,  $\epsilon$ - $\text{LiV}_2\text{O}_5$ , and  $\alpha$ - $\text{V}_2\text{O}_5$ , respectively [34]. It can be seen from the CV curves that the phase conversion from  $\gamma$ - $\text{Li}_2\text{V}_2\text{O}_5$  to  $\delta$ - $\text{Li}_{0.5}\text{V}_2\text{O}_5$  was very weak, implying that the reaction was unlikely to take place. In contrast, the other two phase transitions could occur easily. Similarly, three pairs of CV peaks also appeared for hollow  $\text{V}_2\text{O}_5$  microspheres prepared at a molar ratio of vanadium acetylacetonate to ascorbic acid of 1:10 (Figure 5b). The first pair of peaks was at (2.19, 2.57), (2.24, 2.57), (2.25, 2.57), and (2.27, 2.57) for the corresponding four cycles. The second and third pairs of CV peaks were at (3.15, 3.26) and (3.36, 3.46) for all cycles. However, all the intensities of peaks are weaker than above. Possible lithiation reactions in the  $\text{V}_2\text{O}_5$  cathode may be proposed as follows in Equations (1) and (2).  $\gamma$ - $\text{Li}_2\text{V}_2\text{O}_5$  forms in the first lithiation process. Then,  $\gamma$ - $\text{Li}_2\text{V}_2\text{O}_5$  is converted to  $\alpha$ - $\text{V}_2\text{O}_5$  in the following delithiation process.

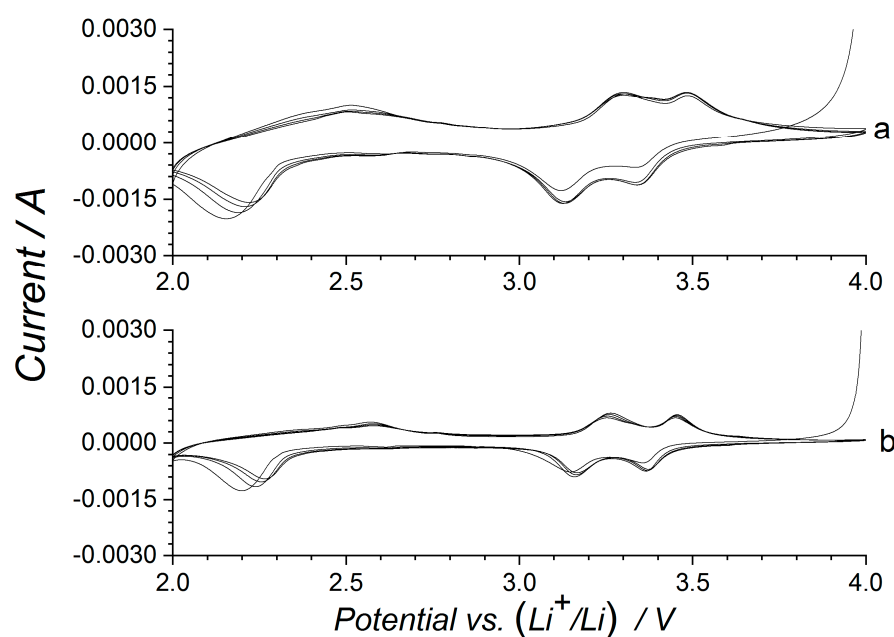
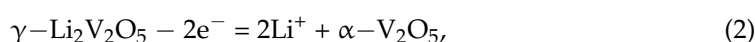
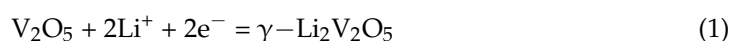


**Figure 5.** Cyclic voltammograms of hollow  $\text{V}_2\text{O}_5$  microspheres prepared at different molar ratios of vanadium acetylacetonate to ascorbic acid: (a) 1:5 and (b) 1:10.

Two types of hollow  $\text{V}_2\text{O}_5$  microspheres were tested as cathode materials for lithium-ion batteries. The 1st, 2nd, and 60th charge–discharge profiles of hollow  $\text{V}_2\text{O}_5$  microspheres at a discharge current density of  $50 \text{ mA g}^{-1}$  are shown in Figure 6a. There was a long discharge platform between 2.25 and 2.35 V, which is ascribed to the formation of  $\gamma$ - $\text{Li}_2\text{V}_2\text{O}_5$  [27]. However, in the following 2nd and 60th cycles, the platform disappeared. The 1st, 2nd, and 60th charge profiles were not the same due to the irreversible phase transitions from  $\gamma$ - $\text{Li}_2\text{V}_2\text{O}_5$  to  $\delta$ - $\text{Li}_{0.5}\text{V}_2\text{O}_5$ ,  $\epsilon$ - $\text{LiV}_2\text{O}_5$ , and  $\alpha$ - $\text{V}_2\text{O}_5$ . The 1st, 2nd, and 60th discharge capacities were  $209.4$ ,  $256.4$ , and  $153.6 \text{ mAh g}^{-1}$ , respectively. Figure 6b shows the cycling performance of hollow  $\text{V}_2\text{O}_5$  spheres at current densities of 50 and  $750 \text{ mA g}^{-1}$ . At a high current density of  $750 \text{ mA g}^{-1}$ , good cycling stability was obtained. The 2nd and 60th discharge capacities were  $151.5$  and  $116.1 \text{ mAh g}^{-1}$ , respectively. The capacity retention rate was 76.6%.



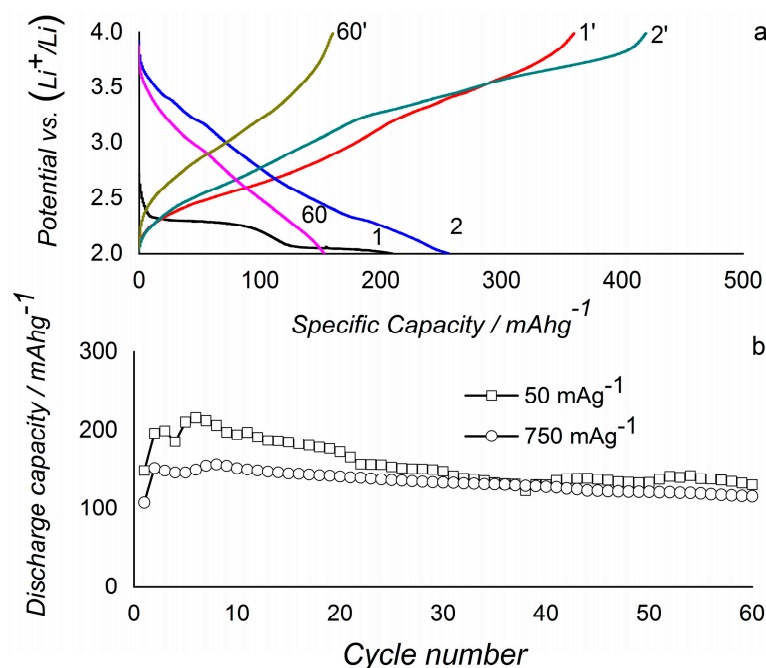


**Figure 6.** The 1st, 2nd, and 60th charge–discharge profiles of hollow  $V_2O_5$  microspheres prepared at a molar ratio of vanadium acetylacetonate to ascorbic acid of 1:5 (a) and its corresponding cycling performance at current densities of 50 and 750  $mA g^{-1}$  (b).

The evolution of the reversible capacity of hollow  $V_2O_5$  microspheres at different current densities was also observed, as shown in Figure 7. Hollow  $V_2O_5$  spheres prepared at a molar ratio of vanadium acetylacetonate to ascorbic acid of 1:5 (Figure 7a) showed higher discharge capacity than those prepared at a molar ratio of 1:10 (Figure 7b). The former could discharge at various current densities of 50, 100, 300, 500, 750, 1000, and 50  $mA g^{-1}$ , while the latter could discharge at lower current densities of 50, 100, 200, 300, 400, 500, and 50  $mA g^{-1}$ . The discharge capacities were 223.6, 208, 170.4, 145.7, 120.4, 119.3, and 115.1  $mA h g^{-1}$  at cycle numbers of 2, 11, 21, 31, 41, 51, and 61. After subsequent discharging at various current densities, the discharge reached a 50  $mA g^{-1}$  current density, and the capacity of the electrode was low, at 115.1  $mA h g^{-1}$ , implying that the rate cycling performance was irreversible. The capacity retention rate was 51.4%. The discharge capacities were 223.6, 208, 170.4, 145.7, 120.4, 119.3, and 115.1  $mA h g^{-1}$  at cycle numbers of 2, 11, 21, 31, 41, 51, and 61. For hollow  $V_2O_5$  microspheres prepared at a molar ratio of 1:10, the discharge capacities are 141.7, 108, 94.9, 78.6, 68.3, 58.7, 50.7, and 68.5  $mA h g^{-1}$  at cycle numbers of 2, 11, 21, 31, 41, 51, 61, and 71. The capacity retention rate was 48.3%. We also compared the performance of various hollow  $V_2O_5$  microspheres discharged above 2.0 V, as shown in Table 1. The electrode of most hollow  $V_2O_5$  microspheres could be cycled at a suitable discharge current density. It is the size of building blocks, not the sphere, that has important effects on the discharge capacity and cycling stability. The hollow  $V_2O_5$  microspheres with nanoparticles, nanoplatelet building blocks, and pores showed high discharge capacity and good cycling stability. However, the cycling performance was not distinguished for well-organized nanospheres. In general, hollow Ni- and graphene-doped  $V_2O_5$  microspheres show the best cycling performance.

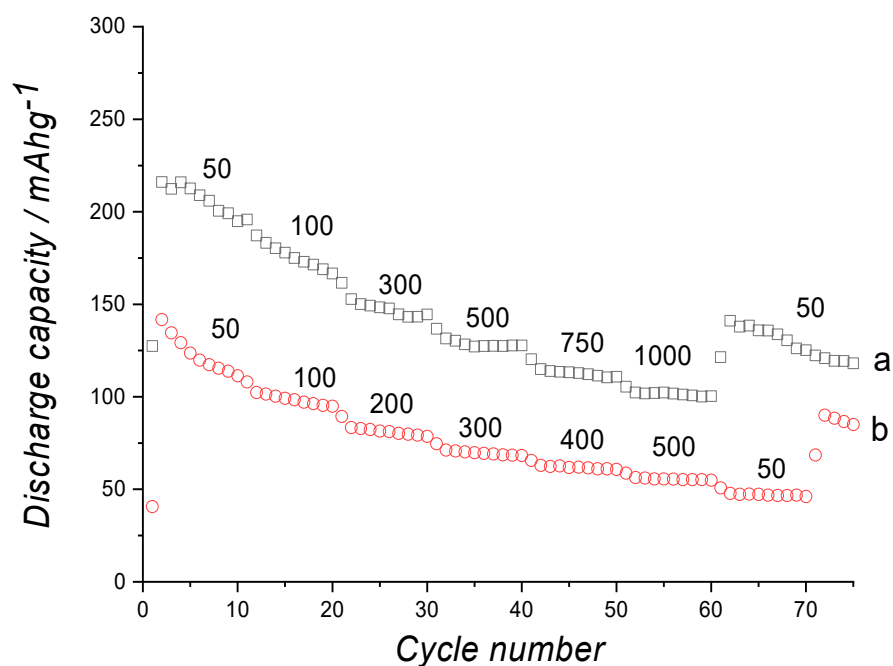


**Figure 7.** The evolution of the reversible capacity at different current densities of hollow  $V_2O_5$  microspheres at different molar ratios of vanadium acetylacetonate to ascorbic acid: (a) 1:5 and (b) 1:10.

**Table 1.** Performance comparison of various hollow  $V_2O_5$  microsphere cathode materials discharged above 2.0 V.

Ref.	Morphologies	Discharge Current Density $mAg^{-1}$	Capacity (Cycle Number) $mAhg^{-1}$
[18]	3.0 $\mu m$ hollow spheres of aggregated 77 nm nanoparticles and an inner diameter of approximately 750 nm	300	190
[20]	4 $\mu m$ hollow Ni-doped $V_2O_5$ microspheres	300	238 (50)
[21]	1 $\mu m$ microspheres built with rod-like nanoparticles	100	282
[27]	4.9 $\mu m$ hollow microspheres with cuboid-shaped building blocks	44.5	287 (40)
[27]	1.3 $\mu m$ hollow microspheres with nanoplatelet-like building blocks	44.5	130 (40)
[22]	22 $\mu m$ hierarchical nanosheet-assembled microspheres	300	243 (200)
[26]	1.4–1.6 $\mu m$ yolk-shell microspheres with 65 nm thick shells	100	194
[34]	400 nm spheres with 65 nm thick shells built with platelike structures	300	266
[29]	7 $\mu m$ porous microspheres	45	160
[24]	1 $\mu m$ hollow microflowers assembled from nanosheets	300	211 (100)
[33]	Approximately 28 nm hollow nanospheres with hollow cavity size of approximately 18 nm	150	181 (50)
This work	1.0 $\mu m$ hollow microspheres built with small rodlike nanoparticles	50	256.4 (2)
		750	151.5 (2)

To elucidate the difference in the electrochemical properties of different hollow  $V_2O_5$  spheres, electrochemical impedance measurements were taken, as shown in Figure 8. The fitted equivalent electrical circuits are also shown in Figure 8.  $R_s$  is active electrolyte resistance.  $C_1$  and  $C_2$  are double-layer capacitance. The impedance of a faradaic reaction is made up of an active charge transfer resistance,  $R_{ct}$ , and a specific electrochemical element of diffusion,  $W$ , called the Warburg element.  $R_f$  is the fixed impedance of the cell [39]. The fitted values of  $R_s$ ,  $R_{ct}$ ,  $R_f$ ,  $W$ ,  $C_1$ , and  $C_2$  were 2.77, 28.81, 12.15, 0.081, 12.15, and  $1.35 \times 10^{-4} \Omega$ , respectively, for hollow  $V_2O_5$  microspheres prepared at a molar ratio of vanadium acetylacetonate to ascorbic acid of 1:5. The fitted values of  $R_s$ ,  $R_{ct}$ ,  $R_f$ ,  $W$ ,  $C_1$ , and  $C_2$  were 3.23, 36.16, 35.96, 0.012, 36.16, and  $5.55 \times 10^{-4} \Omega$ , respectively, for hollow  $V_2O_5$  microspheres prepared at a molar ratio of vanadium acetylacetonate to ascorbic acid of 1:10. It could be observed that hollow  $V_2O_5$  microspheres prepared at a molar ratio of vanadium acetylacetonate to ascorbic acid of 1:5 had a smaller charge transfer impedance than those prepared at a molar ratio of vanadium acetylacetonate to ascorbic acid at 1:5. In addition, the steep slope of the Warburg line for hollow  $V_2O_5$  microspheres prepared at a molar ratio of vanadium acetylacetonate to ascorbic acid of 1:5 relates to the good diffusion capability of lithium ions [40]. This is why hollow  $V_2O_5$  microspheres prepared at a molar ratio of vanadium acetylacetonate to ascorbic acid of 1:5 showed better cycling performance.

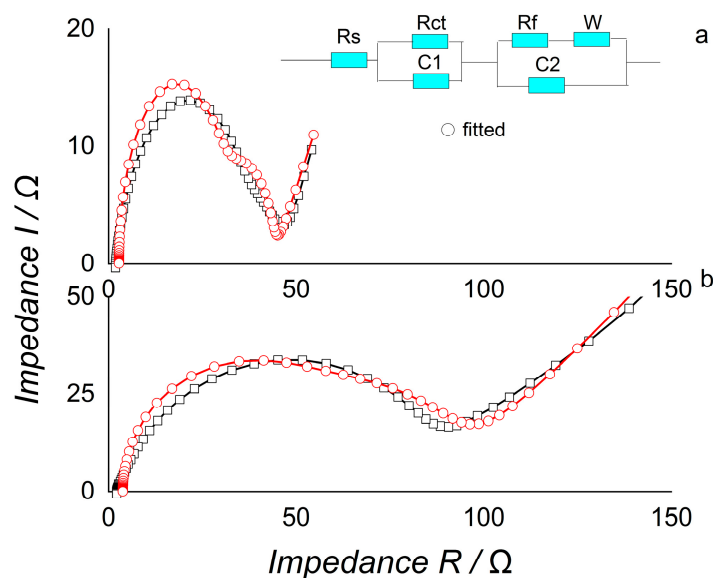


**Figure 8.** Fitted and unfitted Nyquist diagrams of hollow  $V_2O_5$  microspheres prepared at different molar ratios of vanadium acetylacetonate to ascorbic acid: (a) 1:5 and (b) 1:10 (Original data is in black lines, while the fitted data is in red lines).

### 3. Materials and Methods

#### 3.1. Synthesis of Materials

In a simple procedure, 5 mmol ascorbic acid was added to a beaker filled with 30 mL deionized water with magnetic stirring. Then, 1 mmol vanadium acetylacetonate was added to the above clear solution. The mixed solution was further stirred at room temperature. After 2 h, the mixed solution was transferred to a 50 mL Teflon-lined autoclave and kept statically at 200 °C for 24 h. After that, the heating was stopped, and the autoclave was cooled to room temperature. The precipitate in the autoclave was filtered, washed with ethanol, and dried at 80 °C for 6 h. The dried sample was further calcined at 450 °C for 2 h. The molar ratios of ascorbic acid to vanadium acetylacetonate varied between 0:1 and 10:1; the other two samples were prepared under identical conditions.

### 3.2. Characterizations of Materials

All samples were observed with a Hitachi S-4800 field-emission scanning electron microscope (Hitachi Limited, Tokyo, Japan) to obtain the morphological characteristics. X-ray diffraction (PANalytical B.V., Almelo, Nederlanden) patterns were recorded using a diffractometer (CoK $\alpha$ , Analytical, and Pert). Electrode performance was measured with a Land CT2001A battery tester at room temperature. Electrochemical impedance measurements were performed with a Zahner IM6 electrochemical workstation (Zana Company, Kronach, German).

### 3.3. Electrochemical Tests of Hollow V<sub>2</sub>O<sub>5</sub> Microspheres

Hollow V<sub>2</sub>O<sub>5</sub> microspheres were tested as cathode materials for lithium-ion batteries. The composite of positive electrode materials consisted of an active material, a conductive material (superpure carbon), and a binder, polyvinylidenedifluoride, in a weight ratio of 7/2/1. Li metal was used as the counter electrode. The electrolyte was 1 M LiPF<sub>6</sub> in a 1/1/1 (volume ratio) mixture of ethylene carbonate (EC), propylene carbonate (PC), and dimethyl carbonate (DMC). The cells were charged and discharged between 2.0 and 3.5 V voltage limits.

## 4. Conclusions

Hollow V<sub>2</sub>O<sub>5</sub> microspheres of approximately 1 to 2  $\mu$ m were prepared with vanadium acetylacetonate and ascorbic acid involved in the hydrothermal process and calcining treatment. Both were tested as cathode materials for lithium-ion batteries. Well-formed hollow V<sub>2</sub>O<sub>5</sub> microspheres of smaller size showed higher discharge capacity and better cycling stability, which was ascribed to smaller charge transfer impedance. Future work will concentrate on applying amorphous vanadium-based composites to sodium-ion batteries.

**Author Contributions:** Conceptualization, P.W. and H.F.; methodology, P.W.; software, H.F. and L.H.; validation, H.F., P.W. and L.H.; formal analysis, H.F. and P.W.; investigation, L.H. and H.L.; resources, H.F., P.W. and L.H.; data curation, H.F. and P.W.; writing—original draft preparation, H.F., L.H. and H.L.; writing—review and editing, H.F., L.H. and H.L.; visualization, H.F. and L.H.; supervision, H.F. and L.H.; project administration, H.F. and L.H.; funding acquisition, L.H. and H.L. All authors have read and agreed to the published version of the manuscript.

**Funding:** L. He thanks the Youth Science and Technology Fund Project of China Machinery Industry Group Co., Ltd. (QNJJ-ZD-2022-01).

**Data Availability Statement:** Data supporting reported results can be obtained from the correspondence.

**Conflicts of Interest:** Li-Qing He and Hai-Wen Li were employed by the company Hefei General Machinery Research Institute Co., Ltd. The remaining authors declare that the research was conducted in the absence of any commercial or financial relationships that could be construed as a potential conflict of interest. They declare that this study received funding from the Youth Science and Technology Fund Project of China Machinery Industry Group Co., Ltd (QNJJ-ZD-2022-01). The funder was not involved in the study design, collection, analysis, interpretation of data, the writing of this article, or the decision to submit it for publication.

## References

1. Guo, Y.; Wu, S.C.; He, Y.B.; Kang, F.Y.; Chen, L.Q.; Li, H.; Yang, Q.H. Solid-state lithium batteries: Safety and prospects. *eScience* **2023**, *3*, 138–163. [[CrossRef](#)]
2. Liu, B.J.; Li, X.Y.; Zhao, Q.D.; Liu, J.; Liu, S.M.; Wang, S.B.; Tadè, M. Light into the mechanism of photocatalytic degradation of gaseous o-dichlorobenzene over flower-type V<sub>2</sub>O<sub>5</sub> hollow spheres. *J. Mater. Chem. A* **2015**, *3*, 15163–15170. [[CrossRef](#)]
3. McNulty, R.C.; Penston, K.; Amin, S.S.; Stal, S.; Lee, J.Y.; Samperi, M.; Pérez-García, L.; Cameron, J.M.; Johnson, L.R.; Amabilino, D.B.; et al. Self-assembled surfactant-polyoxovanadate soft materials as tuneable vanadium oxide cathode precursors for lithium-ion batteries. *Angew. Chem. Int. Ed.* **2023**, *62*, e202216066. [[CrossRef](#)] [[PubMed](#)]
4. Fei, H.L.; Zhou, H.J.; Wang, J.G.; Sun, P.C.; Ding, D.T.; Chen, T.H. Synthesis of hollow V<sub>2</sub>O<sub>5</sub> microspheres and application to photocatalysis. *Solid State Sci.* **2008**, *10*, 1276–1284. [[CrossRef](#)]
5. Córdoba, R.; Kuhna, A.; Pérez-Flores, J.C.; Morán, E.; Gallardo-Amores, J.M.; García-Alvarado, F. Sodium insertion in high pressure  $\beta$ -V<sub>2</sub>O<sub>5</sub>: A new high capacity cathode material for sodium ion batteries. *J. Power Sources* **2019**, *422*, 42–48. [[CrossRef](#)]

6. Zhu, Y.H.; Zhang, Q.; Yang, X.; Zhao, E.Y.; Sun, T.; Zhang, X.B.; Wang, S.; Yu, X.Q.; Yan, J.M.; Jiang, Q. Reconstructed orthorhombic  $V_2O_5$  polyhedra for fast ion diffusion in K-ion batteries. *Chem* **2018**, *5*, 168–179. [[CrossRef](#)]
7. Trócoli, R.; Parajuli, P.; Frontera, C.; Black, A.P.; Alexander, G.C.B.; Roy, I.; Dompablo, M.E.A.; Klie, R.F.; Cabana, J.; Palacínand, M.R.  $\beta$ - $V_2O_5$  as magnesium intercalation cathode. *ACS Appl. Energy Mater.* **2022**, *5*, 11964–11969. [[CrossRef](#)] [[PubMed](#)]
8. Liu, F.J.; Zhu, Y.T.; Liu, L.Q.; Zhang, Z.; Yu, J.; Cai, J.X.; Yang, Z.Y. Defect-Rich W/Mo-doped  $V_2O_5$  microspheres as a catalytic host to boost sulfur redox kinetics for lithium–sulfur batteries. *Inorg. Chem.* **2023**, *62*, 5219–5228. [[CrossRef](#)]
9. Wang, Z.Q.; Zhou, M.; Qin, L.P.; Chen, M.H.; Chen, Z.X.; Guo, S.; Wang, L.B.; Fang, G.Z.; Liang, S.Q. Simultaneous regulation of cations and anions in an electrolyte for high-capacity, high-stability aqueous zinc–vanadium batteries. *eScience* **2022**, *2*, 209–218. [[CrossRef](#)]
10. Zhang, N.; Dong, Y.; Jia, M.; Bian, X.; Wang, Y.Y.; Qiu, M.D.; Xu, J.Z.; Liu, Y.C.; Jiao, L.F.; Cheng, F.Y. Rechargeable aqueous Zn– $V_2O_5$  battery with high energy density and long cycle life. *ACS Energy Lett.* **2018**, *3*, 1366–1372. [[CrossRef](#)]
11. De, P.; Halder, J.; Priya, S.; Srivastava, A.K.; Chandra, A. Two-dimensional  $V_2O_5$  nanosheets as an advanced cathode material for realizing low-cost aqueous aluminum-ion batteries. *ACS Appl. Energy Mater.* **2023**, *6*, 753–762. [[CrossRef](#)]
12. Kuchena, S.F.; Wang, Y.  $V_2O_5$  intercalated with polyaniline for improved kinetics in aqueous ammonium-ion batteries. *Electrochim. Acta* **2022**, *425*, 140751. [[CrossRef](#)]
13. Minakshi, M. Examining manganese dioxide electrode in KOH electrolyte using TEM technique. *J. Electroanal. Chem.* **2008**, *616*, 99–106. [[CrossRef](#)]
14. Hembram, K.P.S.S.; Kumar, J. Ironation mechanism in vanadium pentoxide ( $V_2O_5$ ) for iron battery application. *J. Phys. Chem. Solids* **2023**, *183*, 11640. [[CrossRef](#)]
15. Liu, N.B.; Zhao, X.Y.; Wang, X.H.; Li, Q.Q.; Wang, L.B. A  $V_2O_5$  cathode for aqueous rechargeable Pb-ion batteries. *Chem. Commun.* **2023**, *59*, 12719. [[CrossRef](#)]
16. Yuan, B.H.; Yuan, X.; Zhang, B.E.; An, Z.; Luo, S.J.; Chen, L.L. Lithium ion batteries cathode material:  $V_2O_5$ . *Chin. Phys. B* **2022**, *31*, 038203. [[CrossRef](#)]
17. Pan, A.Q.; Wu, H.B.; Yu, L.; Lou, X.W. Template-free synthesis of  $VO_2$  hollow microspheres with various interiors and their conversion into  $V_2O_5$  for lithium-ion batteries. *Angew. Chem. Int. Ed.* **2013**, *52*, 2226–2230. [[CrossRef](#)]
18. Fei, H.L.; Li, Z.W.; Feng, W.J.; Liu, X. Stable anode performance of vanadium oxide hydrate semi-microspheres and their graphene based composite microspheres in sodium-ion batteries. *Dalton Trans.* **2015**, *44*, 146–150. [[CrossRef](#)]
19. Uchaker, E.; Zhou, N.; Li, Y.W.; Cao, G.Z. Polyol-mediated solvothermal synthesis and electrochemical performance of nanostructured  $V_2O_5$  hollow microspheres. *J. Phys. Chem. C* **2013**, *117*, 1621–1626. [[CrossRef](#)]
20. Dong, X.L.; Dong, F.Y.; Zhu, K.K.; Li, H.B.; Zeng, S.Y.; Cui, C.S.; Fu, C.G.; Wang, L. Facile preparation of  $V_2O_5$  hollow microspheres with mesoporous on the shell and their electrochemical properties for lithium-ion batteries. *J. Electrochem. Soc.* **2023**, *170*, 170050505. [[CrossRef](#)]
21. Zheng, Y.Z.; Ding, H.Y.; Uchaker, E.; Tao, X.; Chen, J.F.; Zhang, Q.F.; Cao, G.Z. Nickel-mediated polyol synthesis of hierarchical  $V_2O_5$  hollow microspheres with enhanced lithium storage properties. *J. Mater. Chem. A* **2015**, *3*, 1979–1985. [[CrossRef](#)]
22. Yan, B.; Li, X.F.; Bai, Z.M.; Zhao, Y.; Dong, L.; Song, X.S.; Li, D.J.; Langford, C.; Sun, X.L. Crumpled reducedgrapheneoxideconformallyencapsulatedhollow  $V_2O_5$  nano/microsphere achieving brilliant lithium storage performance. *Nano Energy* **2016**, *24*, 32–44. [[CrossRef](#)]
23. Dong, Y.J.; Wei, H.Y.; Liu, W.; Liu, Q.J.; Zhang, W.J.; Yang, Y.Z. Template-free synthesis of  $V_2O_5$  hierarchical nanosheet-assembled microspheres with excellent cycling stability. *J. Power Sources* **2015**, *285*, 538–542. [[CrossRef](#)]
24. Wang, H.E.; Chen, D.S.; Cai, Y.; Zhang, R.J.; Xu, J.M.; Deng, Z.; Zheng, X.F.; Li, Y.; Bello, I.; Su, B.L. Facile synthesis of hierarchical and porous  $V_2O_5$  microspheres as cathode materials for lithium ion batteries. *J. Colloid Interf. Sci.* **2014**, *418*, 74–80. [[CrossRef](#)] [[PubMed](#)]
25. Pan, A.Q.; Wu, H.B.; Zhang, L.; Lou, X.W. Uniform  $V_2O_5$  nanosheet-assembled hollow microflowers with excellent lithium storage properties. *Energy Environ. Sci.* **2013**, *6*, 1476–1479. [[CrossRef](#)]
26. Li, H.K.; Wang, J.X.; Liu, X.; Sun, Q.; Djurisi, A.B.; Xie, M.H.; Mei, Y.; Tang, C.Y.; Shih, K. Template-free synthesis of hierarchical hollow  $V_2O_5$  microspheres with highly stable lithium storage capacity. *RSC Adv.* **2017**, *7*, 2480–2485. [[CrossRef](#)]
27. Liang, X.; Gao, G.H.; Du, Y.C.; Wang, J.C.; Sun, W.; Liu, Y.D.; Zhang, K.; Wu, G.M. Synthesis and characterization of various  $V_2O_5$  microsphere structures and their electrochemical performance. *J. Alloys Compd.* **2018**, *757*, 177–187. [[CrossRef](#)]
28. Shan, Y.L.; Xu, L.; Hu, Y.J.; Jiang, H.; Li, C.Z. Internal-diffusion controlled synthesis of  $V_2O_5$  hollow microspheres for superior lithium-ion full batteries. *Chem. Eng. Sci.* **2019**, *200*, 38–45. [[CrossRef](#)]
29. Qin, H.G.; Chen, L.L.; Wang, L.M.; Chen, X.; Yang, Z.H.  $V_2O_5$  hollow spheres as high rate and long life cathode for aqueous rechargeable zinc ion batteries. *Electrochim. Acta* **2019**, *306*, 307–316. [[CrossRef](#)]
30. Wang, S.Q.; Lu, Z.D.; Wang, D.; Li, C.G.; Chen, C.H.; Yin, Y.D. Porous monodisperse  $V_2O_5$  microspheres as cathode materials for lithium-ion batteries. *J. Mater. Chem.* **2011**, *21*, 6365–6369. [[CrossRef](#)]
31. Cao, A.M.; Hu, J.S.; Liang, H.P.; Wan, L.J. Self-assembled vanadium pentoxide ( $V_2O_5$ ) hollow microspheres from nanorods and their application in lithium-ion batterie. *Angew. Chem. Int. Ed.* **2005**, *44*, 4391–4395. [[CrossRef](#)] [[PubMed](#)]
32. Xue, L.C.; Li, Y.Q.; Lin, W.T.; Chen, F.M.; Chen, G.C.; Chen, D.J. Electrochemical properties and facile preparation of hollow porous  $V_2O_5$  microspheres for lithium-ion batteries. *J. Colloid Interf. Sci.* **2023**, *638*, 231–241. [[CrossRef](#)] [[PubMed](#)]

33. Kim, K.; Lee, M.J. Template-assisted solvothermal assembly of size-controlled hierarchical V<sub>2</sub>O<sub>5</sub> hollow microspheres with tunable nanoscale building blocks and their enhanced lithium storage properties. *Electrochim. Acta* **2017**, *258*, 942–950. [[CrossRef](#)]
34. Sasidharan, M.; Gunawardhana, N.; Yoshio, M.; Nakashima, K. V<sub>2</sub>O<sub>5</sub> hollow nanospheres: A lithium intercalation host with good rate capability and capacity retention. *J. Electrochem. Soc.* **2012**, *159*, A618–A621. [[CrossRef](#)]
35. Shao, J.; Li, X.Y.; Wan, Z.M.; Zhang, L.F.; Ding, Y.L.; Zhang, L.; Qu, Q.T.; Zheng, H.H. Low-cost synthesis of hierarchical V<sub>2</sub>O<sub>5</sub> microspheres as high performance cathode for lithium-ion batteries. *ACS Appl. Mater. Interf.* **2013**, *5*, 7671–7675. [[CrossRef](#)]
36. Yin, Z.D.; Xu, J.; Ge, Y.L.; Jiang, Q.Y.; Zhang, Y.L.; Yang, Y.W.; Sun, Y.P.; Hou, S.Y.; Shang, Y.Y.; Zhang, Y.J. Synthesis of V<sub>2</sub>O<sub>5</sub> microspheres by spray pyrolysis as cathode material for supercapacitors. *Mater. Res. Express* **2018**, *5*, 5036306. [[CrossRef](#)]
37. Hu, P.; Zhu, T.; Ma, J.X.; Cai, C.C.; Hu, G.W.; Wang, X.P.; Liu, Z.; Zhou, L.; Mai, L.Q. Porous V<sub>2</sub>O<sub>5</sub> microspheres: A high-capacity cathode material for aqueous zinc-ion batteries. *Chem. Commun.* **2019**, *55*, 8486–8489. [[CrossRef](#)]
38. Wilkins, P.C.; Johnson, M.D.; Holder, A.A.; Crans, D.C. Reduction of vanadium (V) by L-ascorbic acid at low and neutral pH: Kinetic, mechanistic, and spectroscopic characterization. *Inorg. Chem.* **2006**, *45*, 1471–1479. [[CrossRef](#)]
39. Fei, H.L. Synthesis of hollow nontransparent VO<sub>2</sub> microspheres as stable electrode materials for lithium-ion batteries. *Int. J. Electrochem. Sci.* **2021**, *16*, 210631. [[CrossRef](#)]
40. Sharma, P.; Minakshi, M.; Whale, J.; Jean-Fulcrand, A.; Garnweitner, G. Effect of the anionic counterpart: Molybdate vs. tungstate in energy storage for Pseudo-capacitor applications. *Nanomaterials* **2021**, *11*, 580. [[CrossRef](#)]

**Disclaimer/Publisher's Note:** The statements, opinions and data contained in all publications are solely those of the individual author(s) and contributor(s) and not of MDPI and/or the editor(s). MDPI and/or the editor(s) disclaim responsibility for any injury to people or property resulting from any ideas, methods, instructions or products referred to in the content.